

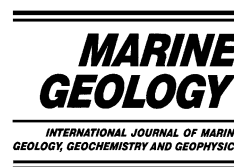


ELSEVIER

Available online at www.sciencedirect.com

SCIENCE @ DIRECT®

Marine Geology 198 (2003) 331–351



www.elsevier.com/locate/margeo

Uptake of elements from seawater by ferromanganese crusts: solid-phase associations and seawater speciation

Andrea Koschinsky^{a,*}, James R. Hein^b

^a International University Bremen, School of Engineering and Science, P.O.Box 750561, D-28725 Bremen, Germany

^b U.S. Geological Survey, 345 Middlefield Rd., MS 999, Menlo Park, CA 94025-3591, USA

Received 3 June 2002; accepted 16 April 2003

Abstract

Marine Fe–Mn oxyhydroxide crusts form by precipitation of dissolved components from seawater. Three hydrogenetic crust samples (one phosphatized) and two hydrothermal Mn-oxide samples were subjected to a sequential-leaching procedure in order to determine the host phases of 40 elements. Those host-phase associations are discussed with respect to element speciation in seawater. The partitioning of elements between the two major phases, Mn oxide and Fe oxyhydroxide, can in a first-order approximation be explained by a simple sorption model related to the inorganic speciation of the elements in seawater, as has been proposed in earlier models. Free and weakly complexed cations, such as alkali and alkaline earth metals, Mn, Co, Ni, Zn, Tl(I), and partly Y, are sorbed preferentially on the negatively charged surface of the MnO₂ in hydrogenetic crusts. The driving force is a strong coulombic interaction. All neutral or negatively charged chloro (Cd, Hg, Tl), carbonate (Cu, Y, Pb, and U), and hydroxide (Be, Sc, Ti, Fe, Zr, Nb, In, Sn, Sb, Te, Hf, Ta, Bi, Th, and Tl(III)) complexes and oxyanions (V, Cr, As, Se, Mo, and W) bind to the slightly positively charged surface of the amorphous FeOOH phase. While coulombic interaction can explain the sorption of the negatively charged species, the binding of neutral species is based on specific chemical interaction. Organic complexation of elements in deep-ocean water seems to be at most of minor importance. Surface oxidation can explain some strong metal associations, e.g. of Co and Tl with the MnO₂ and Te with the FeOOH. Sorption reactions initially driven by coulombic forces are often followed by the formation of specific bonds between the adsorbate and the atoms of the oxide surface. Differences in the associations of some metals between the non-phosphatized and phosphatized hydrogenetic crusts and between the hydrogenetic and the hydrothermal samples reflect the different physico-chemical environments of formation and speciations in oxic seawater vs. less-oxic fluids, especially for the redox-sensitive metals such as Mo and V. These environmental-related differences indicate that the methodology of chemical speciation used here in combination with spectroscopic methods may allow for the detection of changes in paleoceanographic conditions recorded during the several tens of millions of years of crust growth.

© 2003 Elsevier Science B.V. All rights reserved.

Keywords: ferromanganese crust; heavy metal; seawater; speciation; solid-phase association; sequential leaching; surface reactions

* Corresponding author. Tel.: +49-(0)421-2003567;

Fax: +49-(0)421-2003229.

E-mail address: a.koschinsky@iu-bremen.de
(A. Koschinsky).

1. Introduction

Ferromanganese oxyhydroxide crusts (Fe–Mn crusts) occur throughout the ocean floor on sea-

mounts, ridges, and plateaus where currents have kept the rocks swept clean of sediments for millions of years (Aplin and Cronan, 1985; De Carlo et al., 1987; Pichocki and Hoffert, 1987; Usui and Someya, 1997; Hein et al., 2000, and references therein). The Fe–Mn crusts precipitate out of cold, ambient seawater onto hard-rock substrates at water depths of about 400–4000 m. The Fe–Mn crusts are composed of at least three components: manganese oxide, which is intergrown with Fe oxyhydroxide, and minor amounts of detrital minerals such as quartz and feldspar. In addition, thick crusts contain a fourth component, carbonate fluorapatite (CFA), which was incorporated into the crusts during specific periods of diagenesis after the formation of the older parts (pre-middle Miocene) of the crusts (Hein et al., 1993). Other minor phases may also occur in Fe–Mn crusts, such as biogenic or residual biogenic phases.

The Fe and Mn oxyhydroxides acquire significant quantities of elements (e.g. Co, Ni, Pb, Ce, Tl, Te, Pt) from seawater to the extent that the seawater contents of some elements, such as cerium, are controlled by their incorporation into those oxyhydroxides (e.g. Goldberg et al., 1963; Piper, 1974). Fe–Mn crusts grow at very slow rates of 1–10 mm/Ma (mostly 1–6 mm/Ma; Kusakabe and Ku, 1984; Cowen et al., 1993; Segl et al., 1984; Ingram et al., 1990; Eisenhauer et al., 1992; Frank et al., 1999), have a mean porosity of about 60%, and have an extreme specific-surface area that averages 325 m²/g, equivalent to a silica gel. Consequently, the oxyhydroxides reside at the seafloor for long periods of time where metals are incorporated from seawater by adsorption, replacement, and co-precipitation with the major oxides. It has been suggested that the dominant controls on the concentration of elements in crusts include their concentrations in seawater, colloid surface charge, degree of oxidation, types of complexing agents, physical properties, and growth rates (e.g. Li, 1981).

We compare the solid-phase associations of elements in a hydrothermal Mn deposit with those in hydrogenetic Fe–Mn crusts. Hydrogenetic Fe–Mn crusts grade into hydrothermal stratabound

Mn deposits through mixed hydrogenetic–hydrothermal crusts, which gain a greater hydrothermal contribution the closer they form to the hydrothermal source (e.g. Murphy et al., 1991; Hodgkinson et al., 1994; Mills et al., 2001). Both hydrogenetic and mixed hydrogenetic–hydrothermal crusts form at the seafloor. In contrast, hydrothermal Mn deposits form below the seawater–seafloor interface as stratabound layers of Mn oxides or Mn-oxide-cemented clastic rocks. The minor-element content is related to the leaching of basement rock and sediment by the hydrothermal fluids, and trace metals are usually less enriched in hydrothermal deposits than in hydrogenetic crusts.

Simple statistical interelement correlations and factor analyses of bulk analyses have often been used to assess the association of metals in the mineral phases of crusts (Aplin and Cronan, 1985; De Carlo and Fraley, 1992; Bolton et al., 1988). However, for elements that are enriched in more than one phase, the associations are difficult to resolve statistically. Sequential-leaching procedures that dissolve mineral phases of different stability step-by-step have been a useful and widely employed method. Such leaching procedures applied to sediments, soils, and other solids differentiate various hydrogenetic, authigenic, and detrital mineral phases (e.g. Chester and Hughes, 1967; Förstner and Stoffers, 1981; Moorby and Cronan, 1981). Though problems of incomplete selectivity for the discrete phases and variable reproducibility may influence interpretations of sequential-leaching results (Tipping et al., 1985; Kersten and Förstner, 1989), they still find wide application and acceptance because they do provide important genetic information and help solve important environmental questions. Here, a systematic investigation of the leaching partitioning of 40 elements (mainly minor and trace metals) between the main crust mineral phases was carried out. The results are discussed with respect to whether the partitioning in the solid phases determined by leaching generally reflects the speciation of the respective elements in seawater. Our data support and extend the models of others about the mechanisms of chemical precipitation and environmental conditions that existed during crust

growth (Li, 1981; Kusakabe and Ku, 1984; Halbach, 1986).

2. Materials and methods

2.1. Fe–Mn oxyhydroxide samples

Five oxyhydroxide samples were chosen for the leaching experiments (Table 1): a hydrogenetic Fe–Mn crust from the Central Pacific was separated into a younger non-phosphatized layer and an older phosphatized layer (samples CP-1 and

CP-2, respectively); the differentiation between phosphatized and non-phosphatized crust layers was made because earlier work (Koschinsky et al., 1997) showed that phosphatized crusts exhibit a different leaching pattern and different phase associations for some elements. Another hydrogenetic crust (sample NEA-1) from Tropic Seamount in the NE Atlantic is poorer in Mn-phase elements and richer in Fe-phase elements than the Pacific crust (Koschinsky et al., 1995); the sample is not phosphatized. These three hydrogenetic samples consist principally of poorly crystalline Mn oxide (δ -MnO₂ = vernadite), X-ray amor-

Table 1

Origin and bulk chemical composition of the three hydrogenetic crusts CP-1, CP-2 and NEA-1 and of the two hydrothermal oxide samples NFB-1 and NFB-2

Sample	Origin	Cruise/station	Location	Water depth									
CP-1	Central Pacific	SO 66/10DSR	04°10'S, 174°51'W	2000 m									
CP-2	Central Pacific	SO 66/10DSR	04°10'S, 174°51'W	2000 m									
NEA-1	North-east Atlantic	SO 83/116GTV	23°55'N, 20°44'W	1500 m									
NFB-1	North Fiji Basin	SO 99/85DK	16°58'S, 173°55'E	1970 m									
NFB-2	North Fiji Basin	SO 99/85DK	16°58'S, 173°55'E	1970 m									
Sample	As (ppm)	Ba (ppm)	Be (ppm)	Bi (ppm)	Ca (wt%)	Cd (ppm)	Co (ppm)	Cr (ppm)	Cs (ppm)	Cu (ppm)	Ga (ppm)		
CP-1	81.7	1404	0.99	25.0	0.953	2.5	7628	4.8	0.071	408	13.0		
CP-2	31.3	1857	0.74	37.0	7.284	2.9	6192	7.1	0.080	619	15.1		
NEA-1	120.5	1075	2.55	11.5	0.650	1.9	5354	4.5	0.073	110	10.5		
NFB-1	8.8	1765	0.05	0.2	0.649	15.7	29	4.9	0.080	269	17.0		
NFB-2	12.9	2403	0.05	0.1	0.575	12.0	34	5.3	0.074	406	21.2		
Sample	Fe (wt%)	Hg (ppm)	Hf (ppm)	In (ppm)	K (wt%)	Li (ppm)	Mg (wt%)	Mn (wt%)	Mo (ppm)	Na (wt%)	Nb (ppm)		
CP-1	15.16	0.40	5.81	0.076	0.091	3.5	0.45	23.2	630	0.57	20.3		
CP-2	6.83	0.30	3.10	0.086	0.091	4.8	0.44	22.4	671	0.56	38.7		
NEA-1	19.10	0.36	5.90	0.025	0.058	4.0	0.38	15.5	457	0.31	21.4		
NFB-1	0.20	0.07	0.59	0.015	0.296	116.8	2.23	43.8	1538	0.64	1.7		
NFB-2	2.23	0.07	0.34	0.017	0.247	101.5	1.87	40.0	1423	0.60	6.2		
Sample	Ni (ppm)	P (wt%)	Pb (ppm)	Rb (ppm)	Sb (ppm)	Sc (ppm)	Se (ppm)	Sn (ppm)	Sr (ppm)	Ta (ppm)	Te (ppm)		
CP-1	4877	0.49	1371	3.14	10.2	6.0	9.1	2.52	1451	0.64	13.2		
CP-2	8226	3.58	940	2.97	6.8	6.8	9.1	2.65	1412	1.01	12.5		
NEA-1	2367	0.45	1959	1.51	12.0	7.5	8.9	1.59	1502	2.77	12.3		
NFB-1	327	0.07	5	9.36	2.4	3.0	1.5	0.68	665	0.17	1.5		
NFB-2	349	0.08	9	9.33	2.7	3.2	1.9	0.59	557	0.13	1.7		
Sample	Th (ppm)	Ti (ppm)	Tl (ppm)	U (ppm)	V (ppm)	W (ppm)	Y (ppm)	Zn (ppm)	Zr (ppm)				
CP-1	3.4	0.855	196	3.65	596	29.5	40.2	569	609				
CP-2	1.9	0.723	282	2.63	529	29.6	34.4	796	472				
NEA-1	16.7	0.552	109	2.59	875	33.8	36.4	267	483				
NFB-1	0.42	0.004	16.5	0.84	92	1.11	0.78	641	1.6				
NFB-2	0.36	0.007	16.9	1.14	172	0.78	0.85	615	1.9				

In all samples Ag < 50 ppm and Au < 0.1 ppm.

phous Fe-oxyhydroxide, detrital components, and the phosphatized crust layer also contains CFA. The composition of the samples is typical of other hydrogenetic crusts. For comparison with the hydrogenetic precipitates, a hydrothermal Mn-oxide sample from the North Fiji Basin was separated into a harder layer, which according to its mineralogy and chemical composition is purely hydrothermal, and a softer layer, which shows minor hydrogenetic input (labeled NFB-1 and NFB-2, respectively; Kuhn et al., 2003). These samples formed in an environment influenced by reducing hydrothermal solutions, in contrast to the three hydrogenetic samples that grew much slower in oxic deep-sea water. The hydrothermal samples are rich in Mn oxide (todorokite, birnessite) and have low Fe and moderate to low trace-metal concentrations, except Mo, Li, and Ba that are strongly enriched. A more detailed description of the hydrothermal samples is provided elsewhere (Kuhn et al., 2003). Information on the structure of hydrothermal 10Å and 7Å manganates can be found for example in Usui et al. (1989).

2.2. Methods

Two air-dried aliquots were taken from each of the five samples for bulk analysis and two for leaching. Those were used for two identical runs of the leaching procedure and analyses to check reproducibility; presented data are average values (standard deviations within $\pm 4\%$ for the bulk analyses and $\pm 10\%$ for the leaching procedures). No oven drying was carried out in order to avoid changes in phase associations. We adapted known dissolution procedures and combined them into a leaching scheme that had previously been applied to Fe–Mn crusts and nodules, during which reproducibility was determined (Koschinsky and Halbach, 1995). The powdered sample ($< 63 \mu\text{m}$) was put in a 250 ml NALGENE polyethylene bottle, the leaching reagent was added, and the suspension was shaken on a horizontal shaker. The leaching solution was filtered through a 0.45- μm membrane filter and the aqueous phase (including colloids $< 0.45 \mu\text{m}$) was stored for analysis. The solid remaining on the filter was

rinsed twice with deionized water and then immediately transferred to the next leaching step. The pH was checked twice during the leaching and was slightly readjusted, if necessary. The time of the different leaching steps had been shown to be sufficient for the complete dissolution of the respective mineral phases (for the detailed procedure, see Koschinsky et al., 1995). The following four fractions were separated:

L1: adsorbed cations (easily leachable) and carbonate fraction (acid-leachable with acetate buffer);

L2: Mn-oxide fraction (easily reducible);

L3: Fe-oxyhydroxide fraction (moderately reducible);

L4: residual fraction (hardly soluble) with silicates, crystalline oxides, CFA, etc.

For the bulk analyses, 0.2 g of dried crust material was digested by acid-pressure digestion in Teflon bombs. Al, Fe, Ca, P, Mg, Mn, Ba, Sr, Ti, Ni, Co, Zn, Cu, Cr, Mo, V, and Zr were measured with a Leeman ICP–AES spectrometer. Solutions were also analyzed using a Fisons Instrument VG Plasma PQ2 ICP–MS for Sb, As, Ba, Be, Bi, Cd, Cs, Cr, Co, Cu, REEs, Ga, Au, Hf, In, Ir, Pb, Pd, Pt, Mn, Hg, Mo, Ni, Nb, Rb, Re, Rh, Ru, Sc, Se, Sr, Ta, Sn, Te, Tl, Th, W, U, V, Y, Zn, and Zr. A subset of those elements, in addition to Fe, Mn, Na, Al, K, Mg, Ca, Ti, P, and Ag, were analyzed using a ARL 3560 ICP. The same methods used for bulk analyses were also used for analysis of the leaching solutions; however, they had to be adjusted to the different matrices of each leaching solution. For each element, the sum of the amounts released by leaching steps 1–4 was compared with the bulk analysis data to check the recovery; the recovery of the leaching steps with respect to the bulk analyses was between 89% and 110%. Precision was within 7% for replicate analyses of the same solution leaches in which elements have their major associations. With respect to the numerous working steps and difficult matrices, we regard those levels of precision as acceptable. Higher uncertainties for Se due to its low concentrations warrant preliminary interpretations.

For Q-mode factor analysis of the leaching data, each variable percentage was scaled to the

percent of the maximum value before the values were row-normalized and cosine- θ coefficients calculated. Factors were derived from orthogonal rotations of principal-component eigenvectors using the Varimax method (Klovan and Imbrie, 1971). All communalities are ≥ 0.90 .

3. Results

The bulk chemical compositions of the five samples (Table 1) are typical of hydrogenetic crusts and hydrothermal deposits (compare data sets of global crust occurrences in Hein et al., 1997, 2000; Usui and Someya, 1997). The three hydrogenetic samples have Mn (15.5–23.2 wt%) and Fe (6.8–19.1 wt%) as the major elements and high Co, Ni, and other heavy-metal concentrations. The two hydrothermal samples have only Mn as the major element (40.0–43.8 wt%) and show low trace-metal concentrations compared to the hydrogenetic crusts, except for Mo, Ba, and Zn.

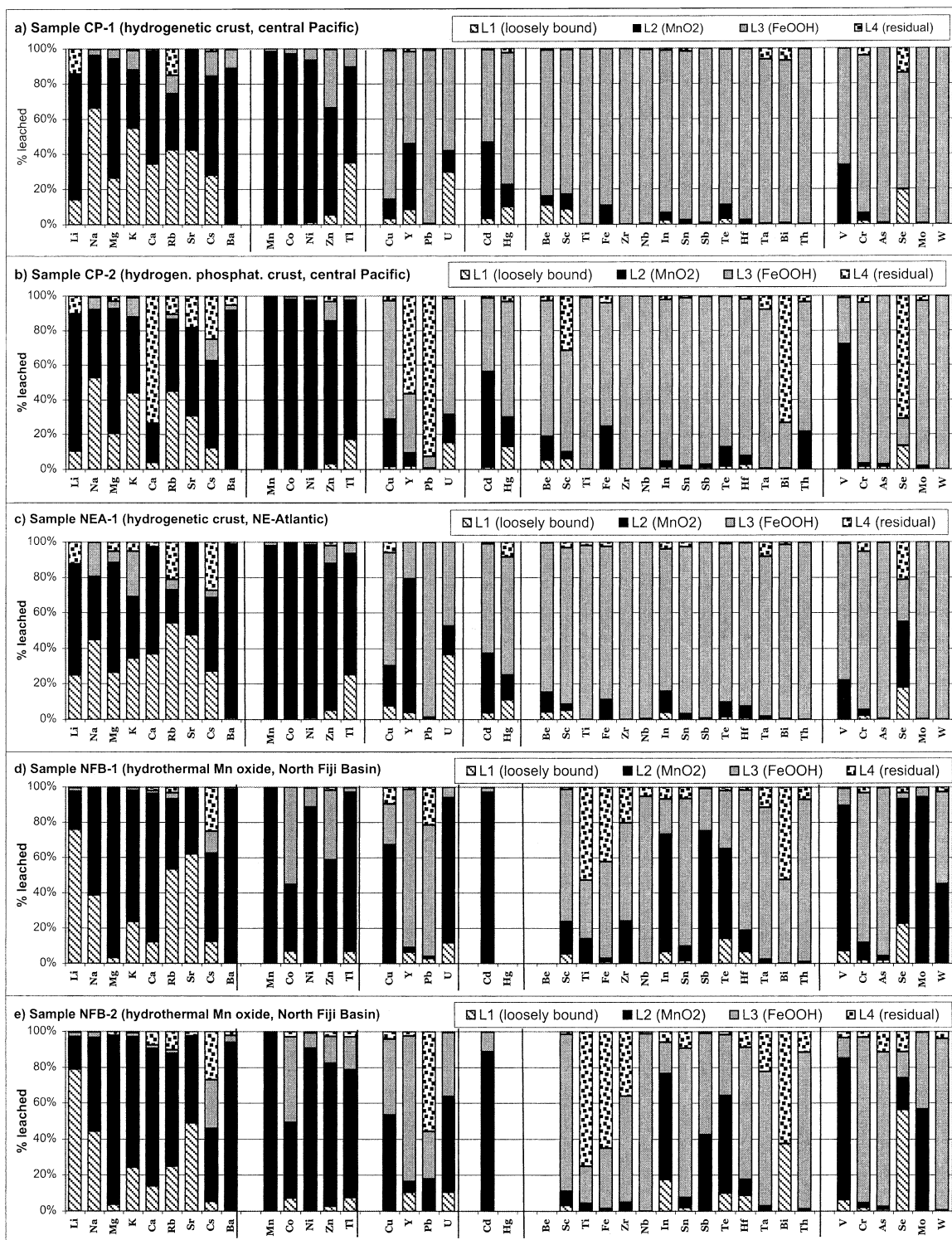
The relative distributions of the elements leached in the four steps L1–L4 (in %) are shown by bar diagrams in Fig. 1a–e. This graphic presentation facilitates comparison of the different crust samples and direct comparison of each element distribution in the leaching fractions with the respective speciation in seawater (see Section 4 for grouping of elements). While the leaching procedure has been shown to be very selective in dissolving the carbonate phase in L1 and Mn oxide in L2, minor amounts of Si and Al were found in L2 and higher Si and Al concentrations in L3 besides their main occurrence in leach L4. A small amount of Fe (10–30%) is associated with L2, due to the intergrowth of the Mn- and Fe-oxide phases. CFA in the phosphatized crusts was not selectively leached within a single leach, but was distributed predominantly in leach L4, with a lesser amount in L3.

A general similarity among the three hydrogenetic crusts (CP-1, CP-2, and NEA-1) and between the two hydrothermal samples (NFB-1 and NFB-2) is obvious (Fig. 1). In the three hydrogenetic crusts, more than 50% of the elements determined show a preferential association with

L3 (FeOOH) followed by L2 (MnO₂). There is a significantly higher amount of many metals in L4 of crust CP-2 compared to the other two. The lesser association of elements with FeOOH in the two hydrothermal samples corresponds to its low concentration (0.2–2.2 wt%; Table 1). Those samples are dominated by Mn oxide, which is reflected by the relatively stronger metal association with L2. However, because most metals are much less concentrated in the hydrothermal deposits than in the hydrogenetic crusts (Table 1), the dominance of associations with L1, L2, and L4 over L3, compared to the hydrogenetic crusts, is only relative.

The first group of elements (alkali and alkaline earth metals) shows a leaching distribution among the fraction of exchangeable plus carbonate-bound metals (L1), the MnO₂ (L2), and to a lesser extent also the FeOOH (L3) and residual fraction (L4). Barium shows a stronger similarity to group 2 elements, the hydrated and weakly complexed cations (Mn, Co, Ni, Zn, and Tl), than with the other alkaline earth metals, because about 80–90% is leached with MnO₂. The carbonate-complexed elements (Y, Pb, Cu, U) show variable distributions among the four leaching fractions; however, in the two non-phosphatized hydrogenetic crusts, associations with FeOOH (L3) predominate, while in the phosphatized crust, Y and Pb are predominantly in the residual fraction (L4), likely hosted by the CFA component of that fraction. The chloro-complexed metals (Hg, Cd, and partly Tl) are predominantly bound in the MnO₂ and/or FeOOH (L2 and L3). The neutral or negatively charged hydroxide complexed metals show a more homogenous association, preferentially bound in FeOOH (L3). The oxyanion group also shows a predominant association with FeOOH, although there are also small complements of V, Mo, and Cr with L1, L2, and L4.

Q-mode factor analysis of the leaching data of the three hydrogenetic crusts confirms the observed associations in the four leaches (Table 2). The results are consistent with element associations that are generally found in typical Fe–Mn crusts from different ocean regions, as demonstrated in Table 2, and emphasize the suitability of the sequential-leaching procedures to investi-



gate the associations of minor and trace elements with the main mineral phases of hydrogenetic crusts. A similar consistency was found for the hydrothermal data sets.

4. Discussion

Information about element speciation in seawater used here is taken from Turner et al. (1981), Byrne et al. (1988), Li (1991), Donat and Bruland (1995), and Byrne (2002), except for elements for which a thorough literature search of recent papers provided additional data. Li (1981, 1991) and Koschinsky and Halbach (1995) showed that it is useful to group the seawater element speciations, such as cations, chloride, hydroxide, and carbonate complexes, and oxyanions, with respect to geochemical behavior and associations with Mn and Fe (hydr)oxides. The charge of the dissolved species appears to be especially important for the sorption on the Mn and Fe phases in that cations are strongly bound to negatively charged MnO_2 surfaces, whereas anions, neutral species, and those with a low-charge density tend to be associated with FeOOH in marine Fe–Mn crusts. Besides inorganic speciation, organic complexes can be important for some metals, especially in shallow-water environments.

We present element speciations in seawater in six groups (Fig. 2a) according to their association with ligands and their charge. Although there is a paucity of information on organic–metal speciation in deep-ocean water for most metals, organic speciation appears to be much less pronounced there compared to surface water environments (see Donat and Bruland, 1995, and discussion below). Consequently, we do not present organic speciation as a discrete group.

The first speciation group consists of the alkali

and alkaline earth elements that in seawater are present predominantly (>85%) as free cations (charge +1 or +2) and behave conservatively in the oceanic water column, having long residence times and limited particle reactivity. The alkali earth metals are also ion paired with SO_4^{2-} (10–14%; Byrne, 2002). The second group consists of the trace metals Mn, Co, Zn, Ni, and Tl, which are also dominated by hydrated cation speciation, but to a minor degree also show chloro, hydroxy, and carbonate complexation and are strongly particle-reactive. Elements of the third group, Y, Pb, Cu, and U, are predominantly carbonate complexes, but they (except U) can also be present in minor amounts as labile complexed cationic species. Group four contains a small number of elements (Cd, Hg, as well as Ag and Au) that are dominated by neutral or negatively charged chloro complexes, such as CdCl_2^0 and HgCl_4^{2-} , but other species (such as CdCl^+) have also been reported to exist; Tl (as TlCl^0) partly belongs to this group. Groups five and six represent the metals strongly hydrolyzed in seawater, being either neutral or negatively charged hydroxide complexes of tri- to hexavalent cations (Sc, Ti, Fe, Zr, Nb, In, Sn, Sb, Te, Hf, Ta, Bi, and Th), or oxyanions (V, Cr, As, Se, Mo, and W). Several metals of group six oxyanions are redox-sensitive and, while prevailing in their more oxidized state (chromate, arsenate, selenate, etc.) in normal oxygenated seawater, can also be present in more reduced forms, either in small amounts in normal seawater (like Cr as $\text{Cr}(\text{OH})_2^+$), or in larger amounts in lower-oxygen seawater environments (like As as arsenite and Se as selenite) (Measures et al., 1984; Sadiq, 1990; Achterberg and Van den Berg, 1997).

A detailed discussion of adsorption and surface-complexation models, such as those by James and Healy (1972), Stumm et al. (1980), Schindler (1981), and Sposito (1983), is beyond the scope of

Fig. 1. Distribution of elements between the four leaching fractions. Key: L1, exchangeable ions plus carbonate; L2, Mn-oxide; L3, Fe-oxyhydroxide; L4, residual fraction. (a) Hydrogenetic sample CP-1. (b) Hydrogenetic phosphatized sample CP-2. (c) Hydrogenetic sample NEA-1. (d) Purely hydrothermal sample NFB-1. (e) Mostly hydrothermal sample NFB-2. The vertical divisions were chosen according to the different major speciation of metals in seawater, as represented in Fig. 2: free cations, Cl-, F-, and OH-complexed cations, carbonate complexes, neutral or negative chloro complexes, hydroxide complexes, and oxyanions.

this paper. The effects of ionic interactions in marine solution chemistry were reviewed by [Millero \(1990\)](#). The specific associations of elements with the Mn and Fe mineral phases of hydrogenetic

Fe–Mn crusts as determined from our leaching experiments can be explained by the chemical models of [Li \(1982\)](#) and [Halbach \(1986\)](#) and are interpreted according to the generalized two-layer

Table 2

Comparison of two highest (X, x) leach percentages for each element if >5% (first sub-column in each column) with Q-mode factor analysis of leach data for each leaching step L1–L4 (second sub-column in each column), and with strong associations of typical Fe–Mn crusts in regional data sets from [Hein et al. \(2000\)](#), and references therein; third sub-column in each column)

	L1			L2			L3		L4			Al-Si +CFA
	L1 = loosely bound+carb.	L1 Q-mode	Biog. crusts	L2 = Mn oxide	L2 Q-mode	Mn crusts	L3 = Fe oxyh.	L3 Q-mode	Fe crusts	L4 = resid.	L4 Q-mode	
Li	x	X		X	X					x	X	
Na	X	X	X	x	X	X						X
Mg	x		X	X	X	X						X
K	X	X		x	X							X
Ca	x		X	X		X				X	X	X
Rb	X	X		x						x	X	
Sr	x	X	X	X	X	X			X			X
Cs	x	X		X	X					x	X	
Ba			X	X	X		x			x		X
Mn				X	X	X						
Co				X	X							
Zn				X	X	X	x					X
Ni				X	X	X	x					
Y				X	X		X	X	X	X	X	X
Pb						X	X	X	X	X	X	
Cu			X	x	X		X	X	X			X
U	x	X		x			X	X				
Cd				X	X	X	X	X				
Hg	x	X		x			X	X				
Tl	x	X		X	X							
Be	x			x			X	X	X			
Sc	x			x			X	X		x	X	
Ti						X	X	X	X			X
Fe				x			X	X	X			X
Ga				X	X		x					
Zr							X	X				
Nb							X	X				
In				x			X	X				
Sn							X	X				
Sb							X	X				
Te				x			X	X				
Hf				x			X	X				
Ta							X	X		x	X	
Bi							X	X		x	X	
Th				x			X	X				
V			X	X	X	X	X	X	X			
Cr							X	X	X	x		X
As							X	X	X			
Se	x	X		X			X			X	X	
Mo						X	X	X				X
W							X	X				

Only leach data of the three hydrogenetic crusts CP-1, CP-2, and NEA-1 are used.

model developed by Dzombak and Morel (1990). The change in the total Gibbs free energy ΔG_{ads} during adsorption of ions on solids is a combination of ΔG of coulombic electrostatic interaction and ΔG of a specific chemical interaction: $\Delta G_{\text{ads}} = \Delta G_{\text{coul}} + \Delta G_{\text{chem}}$. Specific adsorption involves the formation of chemical bonds between the adsorbate and surface Fe or Mn atoms, while coulombic interaction does not involve the formation of chemical bonds, and the sorbing ions and Fe or Mn atoms have a larger distance. The pH_{pzc} (pH of zero point of charge) determines the surface charge of a solid phase at a given pH. For vernadite the pH_{pzc} is 2.8 (Stumm and Morgan, 1996) and for amorphous iron oxyhydroxide in freshwater around 8.5 (Stumm, 1992); the pH of deep seawater is around 8.0. A recent review of points of zero charge for simple (hydro)oxides is given by Kosmulski (2002). For example, goethite in NaCl solution has a pH_{zpc} of 8.5, and ferrihydrite in NaClO_4 has a pH_{zpc} of 7.89–8.7. No data for amorphous FeOOH in seawater could be found. The pH of deep-ocean water may be as low as about 7.1 in places, and it can be reasonably assumed that FeOOH particles may have a slightly positive charge.

For the enrichment of metals in the Mn phase, ΔG_{coul} is the most important term and describes the strong electrostatic interaction of the negatively charged $\delta\text{-MnO}_2$ colloid with hydrated cations, especially transition metals. For adsorption of negatively charged complexes on the slightly positively charged amorphous FeOOH, the ΔG_{coul} term is small but coulombic interaction can still play a role. However, the sorption of neutral compounds on FeOOH is dominated by formation of chemical covalent bonds described by the term ΔG_{chem} (Dzombak and Morel, 1990). This explains why both anions and neutral compounds are associated with FeOOH.

4.1. Leaching distribution in the hydrogenetic non-phosphatized crusts

Here we discuss the applicability of the simple adsorption model for the enrichment of 40 elements in crusts and the suitability of the leaching procedure for the evaluation of metal speciation.

The seawater speciations of the metals (Fig. 2a) are compared with the distribution of the metals in the leaching fractions of the two hydrogenetic non-phosphatized crusts CP-1 and NEA-1 (Fig. 1a,c). In Fig. 2b, the distribution of the elements between only the Mn and Fe phases (L2 and L3) of sample CP-1 is shown to facilitate comparison with speciation of the respective elements in seawater. If the MnO_2 and FeOOH that precipitated from seawater to form the crusts reflect seawater speciation, then cationic and labile complexed metal species should be leached with L2 (MnO_2) while hydroxide and carbonate complexes and oxyanions should be leached with L3 (FeOOH). Neutral and negative chloro complexes should also be found in L3. As a small amount of total Fe (10–30%) was leached with L2 because of the strong intergrowth of Mn and Fe in iron vernadite (Manceau et al., 1992), the metals associated with FeOOH can also show a respective small proportion in L2. As L1 (loosely bound and carbonate) and L4 (residual) mostly represent phases that do not reflect precipitation from seawater, they are not included in the following discussion. To overcome interpretation difficulties arising from the incomplete selectivity of the leaching procedure for some phases and metals, we carried out a factor analysis of the leaching data set (Table 2).

4.1.1. Alkali and alkaline earth metals

The share of Li, Na, Mg, K, Ca, Rb, Sr, Cs, and Ba found in L2 (MnO_2) is consistent with major speciation of these metals as hydrated cations in seawater (Fig. 2). Sato et al. (1989) recognized the mineralogical control on the major element composition and charge-balancing of the cations of marine Fe–Mn-oxide deposits. They found higher concentrations of alkali and alkaline earth metals in Mn oxides precipitated freshly from seawater than in ferric oxides, consistent with our results from the leaching experiments.

4.1.2. Heavy metals with mixed cationic speciation

Manganese is leached to nearly 100% in L2, which corresponds to the cationic speciation (Mn^{2+} and MnCl^+ ; Fig. 2). Cobalt shows the same leaching behavior; it sorbs strongly on the

MnO₂, followed by surface oxidation to Co³⁺ (Murray and Dillard, 1979). If our model is correct, the very small share of Co in L 3 would imply that the percentage of Co as non-cationic species in seawater is smaller than that given by Byrne (2002) (65% Co²⁺, 14% CoCl⁺), but agrees more closely with the data of Pujing and Susak (1991) (CoCO₃⁰ < 1%). However, the results may also simply reflect a greater affinity of Co for MnO₂ which is related to the oxidation of Co(II) to Co(III) on the vernadite surface. For Ni, a speciation of 53% Ni²⁺ and 9% NiCl⁺ has been proposed (Byrne, 2002). Our leaching data suggest that more than 90% of the total dissolved Ni is present as cations. However, small differences (about 10%) found between speciations given in the literature and inferences from our leaching data may simply be a consequence of incomplete selectivity of the leaching procedure, analytical uncertainties, and other reasons such as different sorption behaviors of the various species. For Zn, we again found that the major part is leached in L2, with about 10–25% of Zn in L3. Our leaching data are consistent with the inorganic complexation scheme presented by Stanley and Byrne (1990): 64.3% Zn²⁺, 14.1% ZnCl⁺, 5.7% ZnOH⁺, 10.2% ZnCO₃⁰, 4.9% ZnSO₄⁰, and < 1% other species. Tl exists in seawater in the oxidation states I and III. A species distribution of 61% Tl⁺, 37% TlCl⁰, and minor Tl(OH)₃⁰ and TlCl₄⁻ has been proposed (Byrne, 2002). Flegal and Patterson (1985) suggested that Tl is scavenged as Tl(OH)₃ on Fe–Mn (hydr)oxides; however, Tl(OH)₃⁰ should bind on FeOOH and be leached in L3. Thallium in the crusts is mainly leached in L2, suggesting that Tl may be sorbed on MnO₂ as Tl⁺, which is then likely followed by oxidation to Tl(III) (Li, 1991; Bidoglio et al., 1993). Our results support a strong oxidative enrichment of Tl on MnO₂ (Tl⁺ → Tl³⁺; bulk concentration up to 282 ppm Tl; Table 1), implying that Tl is not a conservative analog to K as suggested by Flegal and coworkers (Flegal and Patterson, 1985; Flegal et al., 1989).

4.1.3. Metals dominated by carbonate speciation

The leaching behavior of Cu (L3 > L2) agrees well with the seawater speciation data of Byrne et

al. (1988) of 80% carbonate speciation and 20% cationic species (Fig. 2), while a newer evaluation by Byrne (2002) gives cationic Cu species a much lower importance. The major Y speciation in seawater is YCO₃⁺ (Byrne, 2002). While the other carbonate-dominated elements in the crusts are leached with L3 (FeOOH), we found a strong association of Y with MnO₂ (L2; 37% for sample CP-1 and 75% for sample NEA-1). This is consistent with the fact that the dominant Y species is positively charged, in contrast to the other heavy-metal carbonate complexes, which are either neutral or negatively charged. The partial association of Y with FeOOH (L3) indicates that negative species such as Y(CO₃)₂⁻ are also important, similar to rare-earth elements which form both mono- and di-carbonato-complexes (Cantrell and Byrne, 1987). Lead carbonate complexes are dominant above pH 7.85 (Byrne, 2002), with chloride complexes being the other important form. The nearly exclusive leaching of Pb with L3 implies a very high proportion of the carbonate complex or other non-cationic species. The major association of U with L3 (FeOOH) is consistent with negatively charged carbonate complexes of the uranyl cation (UO₂(CO₃)₂²⁻, UO₂(CO₃)₃⁴⁻, UO₂(CO₃)₂(HO₂)³⁻; Djogic et al., 1988).

4.1.4. Metals forming neutral or negatively charged chloro complexes

Cadmium speciation is given in the order CdCl₂⁰ > CdCl⁺ > CdCl₃⁻, of which the first and the last species should adsorb preferentially on FeOOH (L3) and the second on MnO₂ (L2). Seawater speciation of Cd (Fig. 2a) and phase associations in the crusts (Figs. 1a,c and 2b) agree very well. The negatively charged chloro complexes of Hg (HgCl₄²⁻ and HgCl₃⁻) are consistent with the major part of Hg being leached in L3. Thallium, which also forms chloro complexes, was already discussed with the cations.

4.1.5. Metals dominated by hydroxide speciation

Byrne (2002) proposed that Be is predominantly a cationic complex with BeOH⁺ > Be(OH)₂. However, about 70–80% is leached with L3 (FeOOH), which suggests the predominance of Be(OH)₂ (and possibly Be(OH)₂CO₃²⁻, as pro-

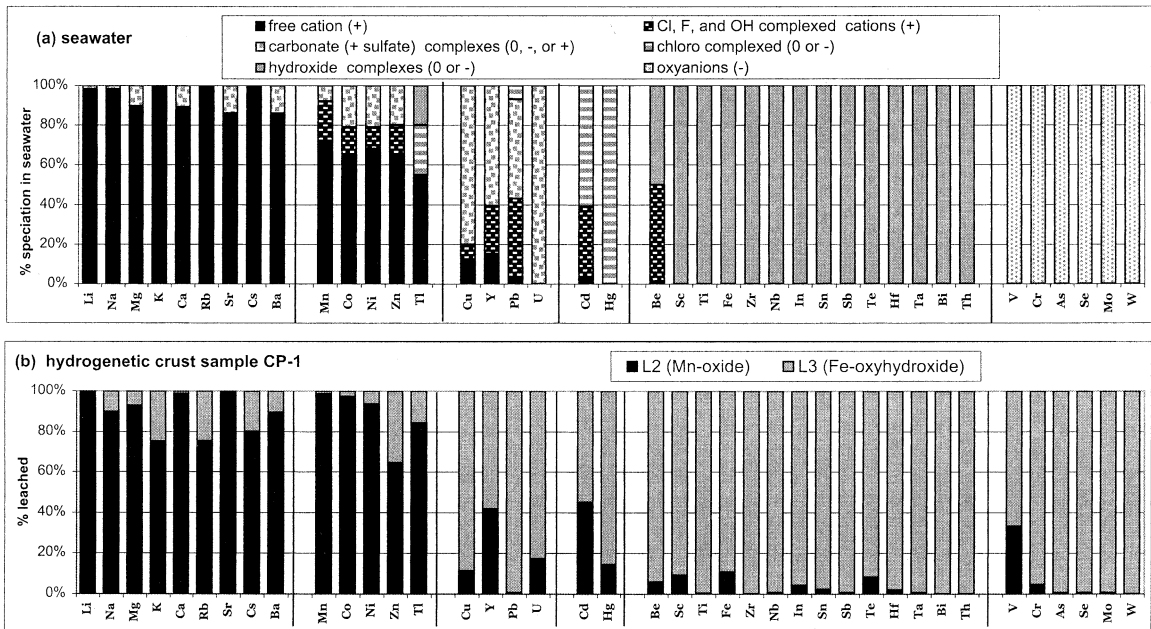


Fig. 2. Inorganic speciation of elements in oxic seawater and grouping of the species (a) in comparison with their associations with MnO_2 and FeOOH in hydrogenetic Fe–Mn crust sample CP-1 (b). The distribution is shown in percent of the total concentration of the element in MnO_2 (L2) and FeOOH (L3). The diagrams demonstrate the similarity between the cationic speciation in seawater and association with the MnO_2 , and neutral and anionic speciation and association with FeOOH .

posed by Bruno, 1990) in seawater. Scandium speciation $\text{Sc}(\text{OH})_3$ is consistent with the leaching distribution $\text{L3} > \text{L2}$, with the small share in L2 attributed to some Fe being in the Mn phase (see discussion above). Also, the $> 95\%$ share of Ti in L3 matches the Ti speciation proposed by Orians et al. (1990) of $\text{Ti}(\text{OH})_4$ or $\text{TiO}(\text{OH})_2$. Titanium is known to be associated with Fe-oxide phases in nature, through specific interactions and through formation of mixed oxide phases, as discussed previously for Fe–Mn crusts by Koschinsky and Halbach (1995). Iron occurs as $\text{Fe}(\text{OH})_3$ in oxic seawater and comprises the FeOOH phase leached by step L3.

Indium, Sn, and Sb speciations ($\text{In}(\text{OH})_3^0$, $\text{SnO}(\text{OH})_3^-$ or $\text{Sn}(\text{OH})_4^0$, and $\text{Sb}(\text{OH})_6^-$) are consistent with $> 80\%$ being leached in L3. Both Te(IV) and Te(VI) species have been reported, for example Li (1991) lists $\text{TeO}(\text{OH})_5^-$, $\text{Te}(\text{OH})_6^0$, and $\text{TeO}(\text{OH})_3^-$. According to Lee and Edmond (1985), Te(VI) in seawater occurs as $\text{Te}(\text{OH})_6^0$ rather than an oxyanion. The main seawater spe-

cies of Te given by Byrne (2002; $\text{TeO}(\text{OH})_5^-$ and $\text{TeO}(\text{OH})_3^-$) and Hein et al. (2003; HTeO_3^- and H_5TeO_6^-) are supported by $> 90\%$ Te being leached with L3. The abundance of hydroxyl groups with these species would probably favor a specific sorption on the FeOOH surface regardless of charge.

While Byrne (2002) indicated that $\text{Zr}(\text{OH})_5^-$ dominates over $\text{Zr}(\text{OH})_4$, Aja et al. (1995) suggested that $\text{Zr}(\text{OH})_4^0$ is the most important species. Because both forms are consistent with Zr being leached to nearly 100% in L3, we cannot discriminate one species over the other. Hafnium is similar to Zr and has been proposed to have both $\text{Hf}(\text{OH})_4^0 > \text{Hf}(\text{OH})_5^-$ speciation (Bruland, 1983) and the opposite (Byrne, 2002), either of which is consistent with $> 90\%$ being leached in L3. Niobium and Ta occur as $\text{Nb}(\text{OH})_6^- > \text{Nb}(\text{OH})_5^0$ and $\text{Ta}(\text{OH})_5^0 > \text{Ta}(\text{OH})_6^-$ in seawater. Sohrin et al. (1998) suggested that both Nb and Ta may form oxyacids, like that of V. Both hydroxide and oxyanion speciations agree with the

leaching behavior of Nb and Ta (90–100% in L3). For Bi, a summary of speciations (Bertine et al., 1996) includes $\text{Bi}(\text{OH})_3$, BiO^+ , and $\text{Bi}(\text{OH})_2^+$. Leaching of >90% with L3 (FeOOH) suggests that the main species is $\text{Bi}(\text{OH})_3$, which agrees with data produced by Byrne (2002). Clegg and Sarmiento (1989) showed the uptake of Bi on Fe oxides and Li (1982) found that Bi is mainly associated with Fe oxides in the ocean, which are also consistent with our leaching results. Thorium speciation of $\text{Th}(\text{OH})_4^0$ is consistent with >95% of the Th being leached in L3, probably reflecting specific interaction of (nearly) uncharged partners.

4.1.6. Elements forming oxyanions

Uptake of oxyanionic elements in marine Fe–Mn concretions was attributed to adsorption on the Fe and Mn oxides by Takematsu et al. (1990), although they did not specify adsorption on which oxide phase. Vanadium as HVO_4^{2-} in seawater (Jeandel et al., 1987) should be mainly sorbed on FeOOH and leached with L3, which does occur for the two hydrogenetic crusts CP-1 and NEA-1 (Fig. 1a,c). Vanadate was shown to form monodentate surface species on oxides (Wehrli and Stumm, 1989). Chromium is leached mostly with L3, consistent with its predominant CrO_4^{2-} speciation (Achterberg and Van den Berg, 1997). Molybdenum in the hydrogenetic samples is leached with L3, which agrees with MoO_4^{2-} speciation in seawater (Sohrin et al., 1999). The partitioning of V and Mo between MnO_2 and FeOOH and seawater is discussed by Takematsu et al. (1985) and Morford and Emerson (1999), among others. Tungsten occurs as WO_4^{2-} in seawater (Sohrin et al., 1999), which sorbs on FeOOH and is leached to >95% in L3. Arsenic, proposed to occur as HAsO_4^{2-} in oxic seawater (Smedley and Kinniburgh, 2002), is consistently leached in L3 (about 90%).

4.1.7. Organic compounds

Recent work (summarized e.g. by Donat and Bruland, 1995) gives organic complexation of metals in seawater a greater importance than did many previous studies. Organic forms of trace metals in seawater include complexes with organic ligands and organometallic compounds in which

the metal is covalently bound to carbon. Voltammetric measurements and modeling of metal complexation in natural waters, including organic ligands, demonstrated that organic complexation can be significant for some metals in seawater, such as Fe, Cu, Zn, and Cd (e.g. Bruland, 1989; Coale and Bruland, 1990; Van den Berg, 1995; Millero, 2001). However, the dominance of organic Cu and Zn complexes over inorganic complexes was found to be restricted to the upper 200–300 m in the northeast Pacific, and concentrations of free hydrated Cu^{2+} and Zn^{2+} ions increased up to 2000-fold below that water depth due to the marked decrease of organic ligand concentrations (Bruland, 1989; Coale and Bruland, 1990). It is reasonable to assume for other metals that organic compounds are also negligible in deep-ocean water. Because Fe–Mn crusts generally form at water depths greater than 1000 m, our hypothesis is that inorganic-metal complexation is significantly more important than organic compounds with respect to incorporation and enrichment of metals in crust phases.

Biomethylation has been found for Sb, As, Ge, Sn, Pb, Cd, Hg, and Tl, which forms metal-organic compounds such as $\text{Me}_2\text{Pb}^{2+}$, MeCd^+ , Me_2Hg , and Me_2Tl^+ in the ocean (e.g. Schedlbauer and Heumann, 2000, and references therein). Whether such compounds play a role in the association of the metals with the different mineral phases in the crusts is difficult to ascertain. First, data on the distribution and relative importance of organometallic compounds are scarce. Second, it is not known what the surface charge of these complexes in seawater would be – for example, Me_2Tl^+ would sorb on the Mn-oxide surface as a cation, whereas a respective chloro complex such as $\text{Me}_2\text{Tl}(\text{Cl})^0$ would preferentially bind on the Fe-oxyhydroxide surface. If methyl compounds in seawater play a significant role and are present mostly as cations, this could explain why we find somewhat more Tl in the L2 leach of the Mn-oxide phase than pure inorganic speciation would warrant.

Also the role of organic ligands and organic coatings in modifying inorganic surface properties has to be taken into account (Au et al., 1999). It was suggested that sorption of organic ligands on

oxide surfaces can result in a negative surface charge for all particles in seawater (Balistrieri et al., 1981). However, this is only possible if sufficient amounts of suitable ligands are available. Suitable ligands are available in the upper few hundred meters of the ocean water including estuarine and coastal waters (Hunter and Liss, 1979), however, it is not likely that the surface charge on the Mn and Fe oxides in deep-ocean water are significantly modified by organic ligands. The concentration of dissolved organic matter in the deep-ocean water is low (François et al., 2002; Fry et al., 1996) and the organic-carbon content in crusts is extremely low (Hein, unpubl. data).

4.1.8. Metals displaying more than one oxidation state in marine environments

Dissolved Cu, Hg, Tl, Fe, Sb, Te, V, Cr, As, Se, and Mo can be present in seawater in more than one oxidation state (e.g. Andreae, 1986; Donat and Bruland, 1995; Byrne, 2002). In general, the more oxidized species, such as Cu(II), Cr(VI), and As(V), prevail in oxic seawater, and only for Tl does the lower oxidation state of Tl(I) seem to be more abundant (Flegal et al., 1989; Byrne, 2002). Cobalt, which in the dissolved state is always Co(II), can be surface-oxidized to Co(III) after adsorption. Mercury, Sb, Te, V, Cr, As, Se, and Mo were found to be associated with the FeOOH in our leaching experiments with the hydrogenetic samples, which is explainable by their anionic speciation in seawater. Copper occurs in both the Mn and Fe phases, in agreement with its mixed speciation. These partitionings show that generally the redox-sensitive metals are distributed between the Mn and Fe phases according to the charges of their seawater complexes.

However, we think that oxidative surface enrichment may explain why some of the metals show a stronger association with a certain phase than the dissolved speciation would imply. For a few elements, the enrichment process on crusts has been attributed to surface oxidation on MnO₂, such as for Co and Tl (Murray and Dillard, 1979; Bidoglio et al., 1993). We found that about 98% of the oxide-bound Co and about 85% of oxide-bound Tl are with the MnO₂ (Fig. 2b),

while the cationic seawater speciation of Co and Tl is reported to be only 79% and 61%, respectively (Fig. 1; Byrne, 2002). Surface oxidation strongly enhances the enrichment of a metal on the oxide surface, explaining the high share of Co and Tl in the Mn phase. Coordinated surface OH groups are able to mediate electron transfer from metal ions to the oxygen molecule (Wehrli et al., 1989); thus metal sorption by formation of inner-sphere complexes on both MnO₂ and FeOOH can catalyze oxidation. The oxidation of As(III) on both Mn(IV) and Fe(III) oxides in aquatic systems has been observed (e.g. Oscarson et al., 1981; De Vitre et al., 1991). Belzile et al. (2001) found that Sb(III) reacted similarly to As(III) in that antimonite was rapidly and completely oxidized to Sb(V) after adsorption on Fe and Mn oxyhydroxides. Dissolved oxygen alone did not oxidize Sb(III) within the time of the study. Hein et al. (2003) found that Te is likely oxidized on the surface of FeOOH.

4.2. Differences in element distributions in the phosphatized crust

Crust sample CP-2 was impregnated with CFA under less-oxic conditions than extant during oxide precipitation. Puteanus and Halbach (1984) postulated that in addition to the diluting effect of CFA, partial dissolution and recrystallization of the crust material took place during phosphatization. Most elements show a similar leaching distribution as for the non-phosphatized crusts in the four leaching fractions L1–L4. Some metals, however, have a much different leaching pattern in the phosphatized crust. The CFA, which is mostly leached in L4, hosts not only Ca, but also Pb, Bi, Sc, Y, and Se (Fig. 1b). CFA with heavy metals in the structure and base-metal phosphates have the highest stability with respect to reducing and acidic solutions (Nriagu, 1984), which explains why the metal-rich CFA fraction was leached predominantly in L4. The CFA has an open lattice that allows a great number of diadochic substitutions. Ca²⁺ in the apatite structure can be substituted by a number of other elements, including Sc³⁺, Y³⁺, and Bi³⁺ (Nathan, 1984). The PO₄³⁻ in the apatite lattice can be substituted

by other anions, most commonly CO_3^{2-} , SO_3^{2-} , F^- and Cl^- ; though Nathan (1984) did not list selenate, which we found in the CFA leach, it should also be compatible with the apatite structure. We also found increased concentrations of Mg, Sr, Ba, Cs, and some Cu and Zn in leach L4 of the phosphatized sample, indicating association of these metals with apatite. For Pb, formation of less-soluble phosphate phases, such as pyromorphite, has been proposed (Koschinsky et al., 1997). Consequently, for the metals listed, the element distributions in phosphatized crusts do not reflect the original seawater speciation because phosphatization was a secondary process that changed the metal associations after their initial precipitation from seawater.

In contrast to the non-phosphatized crusts, most V is leached with L2 in the phosphatized crust instead of being leached with L3. This possibly indicates that a species less oxidized than HVO_4^{2-} predominated under the suboxic conditions that prevailed during crust phosphatization and was thereby bound to MnO_2 . A possible species is VO^{2+} , which has been shown to become specifically adsorbed on hydrous oxides (Wehrli and Stumm, 1989). This oxocation would sorb on the MnO_2 surface according to our model, forming inner-sphere bidentate surface complexes (Wehrli and Stumm, 1989). Furthermore, the rate of oxygenation of VO^{2+} is significantly enhanced by adsorption on hydrous oxide surfaces (Wehrli and Stumm, 1989), which may indicate another oxidation reaction that occurs on crust phases.

4.3. Differences in element distributions in hydrothermal samples

Two important differences between the hydrogenetic- and hydrothermal-oxide samples can be regarded as important with respect to association of trace metals: the dominance of todorokite and birnessite over vernadite and the low content of Fe oxyhydroxide in the hydrothermal samples. The pH_{zpc} for birnessite and todorokite are in the same range as that of vernadite, giving them strong negative surface charges in seawater and dilute hydrothermal fluids. Tripathy et al. (2001) determined the pH_{zpc} to be between 1.8 and 2.2

for birnessite, which is consistent with older data (e.g. 2.2 by Balistrieri and Murray, 1982; 1.8 for todorokite by Murray et al., 1968). The low-Fe content results in generally lower amounts of anionic and neutral metal species in leach L3 compared to the hydrogenetic samples. Differences in metal speciations in normal seawater and hydrothermally influenced waters that typically have pH and Eh values lower than seawater will be especially pronounced for elements with pH dependent speciation, such as carbonate complexes, strongly hydrolyzed metals, and redox-sensitive elements.

The generally higher alkali and alkaline earth metal concentrations in the hydrothermal samples NFB-1 and NFB-2 (Table 1) reflect the strong enrichment of these elements in hydrothermal fluids (e.g. Von Damm, 1995). They are mostly distributed between L1 (loosely bound plus carbonate phases) and L2 (Mn oxide; Fig. 1d,e). The only striking difference compared to the hydrogenetic crusts is the strong enrichment of Li in L1 of the hydrothermal samples, which indicates either a large amount of loosely bound Li, or a discrete Li phase. According to Kuma et al. (1994), alkali metals are readily incorporated into phyllosulfates, which are typical of hydrothermal Mn deposits; we suggest that these may be the host phases for Li in our samples as well. The easy exchangeability of Li could be explained by its small ionic radius (0.68 Å) compared to the other alkali cations (Cs 1.67 Å), which might facilitate a removal of the Li cations from the interstices of the crystal structure.

Similar to the phosphatized crust CP-2, most V is leached with L2 in hydrothermal samples (Fig. 1d,e), possibly again indicating a species less oxidized than HVO_4^{2-} in reducing hydrothermal fluids that binds to the todorokite/birnessite. The reduced V(IV) vanadyl species VO^{2+} and $\text{VO}(\text{OH})^+$ (Wehrli and Stumm, 1989) would bind to the Mn oxide because of their positive charge. A shift from leach L3 to L2 is also evident for Mo, which is associated with FeOOH in all three hydrogenetic samples, but is leached 100% with the Mn oxide in the purely hydrothermal sample NFB-1. Glasby et al. (1997) suggested that Mo is scavenged by Mn oxide in hydrothermal deposits.

The hydrothermal sample NFB-2 with some hydrogenetic component shows about 30% Mo in L3. This may reflect a different speciation of Mo in oxic seawater and in reducing hydrothermal fluids. Molybdenum in these Mn deposits is predominantly present as an octahedrally coordinated polymolybdate species as shown by X-ray absorption spectroscopy (Kuhn et al., 2003). The todorokite structure would allow Mo^{6+} to substitute for Mn^{4+} in the Mn(IV)O_6 -octahedra since their ionic radii are similar (Mn^{4+} : 0.62 Å, Mo^{6+} : 0.68 Å). Molybdenum may also occupy hydrated interlayer sites and its ligand oxygen and hydroxyl ions would be shared with the anionic Mn lattice (Giovanolli and Arrhenius, 1988).

Chromium, which in hydrothermal fluids is dominantly Cr(III), such as Cr(OH)_2^+ , Cr(OH)_3^0 (Byrne, 2002), or organically complexed species (Sander and Koschinsky, 2000), would be leached in L3, making the last two indistinguishable from chromate. The same is probably true for the less-oxidized forms of Sb, As, and Se that may prevail in hydrothermal fluids. Arsenic(III) and Sb(III) species like As(OH)_3^0 , As(OH)_4^- , HAsO_2^0 (Sadiq, 1990), and Sb(OH)_3 (Byrne, 2002) that may exist in hydrothermal fluids would also adsorb preferentially on FeOOH and be leached in L3, as are HAsO_4^{2-} and Sb(OH)_6^- . Also, Se(IV) as SeO_3^{2-} has a higher affinity for amorphous FeOOH than for MnO_2 . However, sorption on the latter is also possible (Balistrieri and Chao, 1990), especially when only minor FeOOH is available, as in the hydrothermal sample NFB-1 in which Se was mostly leached with L2 (Fig. 1d). When the higher energy sites of FeOOH are absent, other highly surface-active phases (here todorokite and birnessite) become the primary sorbent. Also, oxidation of the reduced species from the hydrothermal fluids on the oxide surfaces, as described in Section 4.1.8, is likely to occur during the formation of hydrothermal deposits that form in the mixing zones of reducing hydrothermal fluids and cold oxic seawater.

Interestingly, Co that is completely associated with MnO_2 in the hydrogenetic crusts, does not show such a strong association in the hydrothermal samples (Fig. 1d,e). Co^{2+} is not incorporated in the todorokite phase, as was also determined

by microprobe analyses of todorokite laminae in crusts (Koschinsky et al., 1997), and is probably not enriched by surface oxidation on the MnO_2 , as it does in hydrogenetic crusts. Also, Y is not significantly associated with the Mn phase, in contrast to the hydrogenetic samples, implying a different speciation in low-temperature hydrothermal fluids than in ambient seawater.

4.4. Assessment of the method and model

While the reported metal speciations in seawater and the element associations observed in our leaching experiments are generally consistent with our first-order electrostatic model, inconsistencies are observed for a few elements. Part of these differences may be due to the limitations of the leaching method, including constraints on precision, partly incomplete selectivity of the individual leaches, and the fact that several elements are associated with two or more phases that are leached in different steps. Spectroscopic studies using methods such as X-ray Photoelectron Spectroscopy (XPS), Extended X-ray Absorption Fine Structure Spectroscopy (EXAFS), and X-ray Absorption Near Edge Structure Spectroscopy (XANES) might provide important additional information about the nature of metal incorporation in the crusts and help to make the interpretation of sequential-leaching procedures more quantitative. However, these methods usually require rather high concentrations of the sorbate, much higher than present in crusts. Therefore, some minor and trace elements cannot be investigated at naturally occurring concentrations, and the applicability of experimental results with higher concentrations to the natural system remains unclear.

5. Summary and conclusions

Three hydrogenetic Fe–Mn crust samples and two hydrothermal Mn-oxide samples were sequentially leached and the distribution of the elements in the various leached phases are related to their speciation in seawater. The distribution of 40 elements in the leaches of MnO_2 and FeOOH in

hydrogenetic crusts reflects, to a first-order approximation, the inorganic speciation of the elements in seawater in which the crusts formed, and supports and extends previously developed models of trace-metal incorporation into Mn and Fe oxides. Free cations and weakly complexed cations, such as alkali and alkaline earth metals, Mn, Co, Ni, Zn, Tl, and partly Y, are sorbed preferentially on the negatively charged surface of MnO₂ (vernadite) in hydrogenetic crusts; the driving force is a strong coulombic interaction. This first step of metal-oxide association is often followed by the formation of chemical bonds between the sorbed metal species and the atoms of the Mn- or Fe-oxide surface. For example, our model suggests that Tl seawater speciation is mostly Tl⁺ rather than Tl(OH)₃ and Tl is strongly (probably oxidative) enriched on MnO₂. While the first determining step is coulombic adsorption of Tl⁺, the surface oxidation probably requires the formation of chemical bonds between the Tl atom and the atoms of MnO₂. Surface oxidation may also explain why Co and Tl show a somewhat stronger association with the Mn phase than the seawater speciation distribution would imply.

All neutral and negatively charged metal complexes bind to the amorphous FeOOH; these are the chloro complexes of Cd and Hg, the carbonate complexes of Cu, Pb, U (and Y), the hydroxide complexes of Be, Sc, Ti, Fe, Zr, Nb, In, Sn, Sb, Te, Hf, Ta, Bi, and Th, and the oxyanions of V, Cr, As, Se, Mo, and W. The coulombic interaction may still play a role in the sorption of anionic species on the slightly positively charged FeOOH surface, but the binding of neutral species on the FeOOH surface with low-charge density is driven by specific chemical interactions. Organic complexation is not likely to play an important role in the distribution of the metals between the oxide phases. The metal association patterns for the Atlantic and Pacific crusts are very similar, despite variations in bulk compositions.

Phosphatization changed the solid-phase association of Ca, Sr, Y, Sc, V, Se, Pb, and Bi, which reflects the different seawater speciation of those elements during phosphatization compared to times of oxide accretion. These metals (except

V) were likely transferred to the apatite phase (Hein and Morgan, 1999; Hein and Koschinsky, unpubl. data). For V, VO²⁺ is suggested as the likely seawater species (rather than HVO₄²⁻) to exist in the suboxic environment that characterized phosphatization. In hydrothermal samples, todorokite and birnessite form the major Mn-oxide phases and host the trace metals. Differences in the solid-phase associations between the hydrogenetic crusts and the hydrothermal samples reflect the different physico-chemical environments and the different speciations of some metals in ambient oxic seawater and less-oxic to reducing hydrothermal fluids. This is most pronounced for Mo and V, which are associated mainly with the FeOOH phase in the hydrogenetic crusts, but mainly with the MnO₂ phase in the hydrothermal samples. Also, the different solid-phase properties of the hydrothermal crystalline todorokite and birnessite compared to the poorly crystalline vernadite, and the absence of sufficient Fe phases for significant metal scavenging, contribute to the observed metal distributions.

The sequential-leaching procedure used is a viable method for separating the two major phases of crusts that precipitate from seawater, MnO₂ and FeOOH, and the minor and trace metals associated with them. Because the solid-phase associations in a first-order approximation reflect the seawater speciation of the elements at the time of crust precipitation, sequential leaching in combination with spectroscopic studies such as EXAFS may be useful for identifying speciation changes associated with paleoceanographic environmental changes that occurred during the tens of Ma of crust growth. Also, hydrothermal influence can be recognized by the different metal associations.

Acknowledgements

All samples were recovered during different research cruises of the R/V *Sonne* funded by the German Bundesministerium für Bildung und Forschung; SO 66 (Project No. 03 R 398), SO 83 (Project No. 03 R 424), and SO 99 (Project No. 03 G 0099 A). Thanks are due to U. Müller, C.

Arndt and B. Alberts for the experimental and analytical work, J. Dowling for technical support, and A. Foster for discussions. An earlier version of the manuscript profited from the helpful comments of others. We are indebted to Akira Usui and an anonymous reviewer for useful reviews.

Appendix

Percentage distribution of elements in the four leaches L1–L4 of the three hydrogenetic crusts CP-1, CP-2, and NEA-1, and the two hydrothermal samples NFB-1 and NFB-2

	L1 (%)	L2 (%)	L3 (%)	L4 (%)	L1 (%)	L2 (%)	L3 (%)	L4 (%)	L1 (%)	L2 (%)	L3 (%)	L4 (%)	L1 (%)	L2 (%)	L3 (%)	L4 (%)	L1 (%)	L2 (%)	L3 (%)	L4 (%)
	CP-1	CP-1	CP-1	CP-1	CP-2	CP-2	CP-2	CP-2	NEA-1	NEA-1	NEA-1	NEA-1	NFB-1	NFB-1	NFB-1	NFB-1	NFB-2	NFB-2	NFB-2	NFB-2
Li	14.3	71.4	0.0	14.3	10.4	79.2	0.0	10.4	25.0	62.5	0.0	12.5	76.0	21.4	2.1	0.4	78.8	18.2	2.5	0.5
Na	66.3	29.8	3.5	0.4	52.9	39.3	7.1	0.7	44.8	35.5	19.4	0.3	38.7	60.4	0.6	0.3	44.5	52.0	3.4	0.2
Mg	26.5	67.8	5.4	0.3	20.6	72.0	4.4	3.0	26.7	61.6	6.4	5.3	3.1	96.3	0.3	0.3	3.7	93.7	0.3	2.3
K	54.9	33.0	11.0	1.1	44.0	44.0	11.0	1.1	34.5	34.5	25.9	5.2	23.6	74.3	1.7	0.3	24.3	72.9	2.0	0.8
Ca	34.6	63.0	1.0	1.3	4.0	22.4	0.2	73.4	36.9	60.0	0.5	2.6	12.3	84.0	1.6	2.1	13.9	76.5	2.0	7.6
Rb	42.7	31.8	10.5	15.0	45.1	41.4	2.7	10.8	54.3	18.5	6.0	21.2	53.6	39.7	3.3	3.3	25.0	62.7	1.9	10.4
Sr	42.7	56.9	0.1	0.3	30.8	50.6	0.2	18.4	47.7	51.3	0.3	0.7	62.1	37.6	0.0	0.3	49.0	48.5	0.2	2.3
Cs	28.2	56.3	14.1	1.4	12.5	50.0	12.5	25.0	27.4	41.1	4.1	27.4	12.5	50.0	12.5	25.0	5.4	40.5	27.0	27.0
Ba	0.8	88.0	10.7	0.6	0.4	91.3	3.1	5.2	1.1	97.2	0.4	1.3	0.5	98.0	1.1	0.3	0.4	93.6	3.8	2.2
Mn	0.0	98.3	1.7	0.0	0.0	99.0	0.8	0.2	0.0	97.7	2.3	0.0	0.0	99.5	0.5	0.0	0.0	99.6	0.4	0.0
Co	0.7	96.4	2.9	0.0	0.5	97.5	1.8	0.1	0.5	98.8	0.7	0.0	6.9	37.9	55.2	0.0	7.5	41.8	47.8	3.0
Zn	5.6	60.6	33.2	0.6	3.3	82.3	11.2	3.3	5.3	82.6	10.1	2.1	1.1	57.8	39.5	1.6	2.6	79.7	15.1	2.6
Ni	1.2	92.3	6.5	0.0	0.4	96.9	2.2	0.4	1.1	97.2	1.6	0.1	0.2	88.7	10.7	0.4	0.2	90.6	8.6	0.6
Y	8.6	37.3	52.3	1.8	2.1	7.3	34.3	56.4	3.9	75.1	20.9	0.1	6.4	2.6	89.7	1.3	10.6	5.9	81.2	2.4
Pb	0.1	0.5	98.5	0.9	0.1	0.7	6.7	92.5	0.0	1.1	98.5	0.3	2.7	1.2	74.6	21.5	0.3	17.5	26.4	55.7
Cu	3.4	10.8	84.6	1.2	1.9	26.8	68.4	2.9	7.6	22.7	63.8	5.9	0.7	66.5	23.3	9.4	0.5	52.9	42.6	4.1
U	29.8	12.0	58.2	0.0	15.6	16.0	66.9	1.5	36.7	15.8	47.5	0.0	11.8	82.3	5.9	0.1	10.5	53.3	35.8	0.4
Cd	3.6	43.0	52.6	0.8	1.4	54.9	42.4	1.4	3.7	33.5	61.8	1.0	0.2	96.9	2.8	0.1	0.5	88.2	11.1	0.2
Hg	10.0	12.5	75.0	2.5	13.3	16.7	66.7	3.3	11.1	13.9	66.7	8.3	–	–	–	–	–	–	–	–
Tl	35.1	54.5	10.3	0.1	17.3	80.1	2.5	0.2	25.2	68.3	6.0	0.5	7.0	89.9	2.8	0.3	7.7	71.1	18.2	3.0
Be	11.0	5.0	83.0	1.0	5.4	13.5	78.4	2.7	4.3	11.0	84.3	0.4	–	–	–	–	–	–	–	–
Sc	8.7	8.3	82.2	0.8	6.2	3.7	58.7	31.5	5.3	3.3	88.0	3.3	5.4	18.3	74.9	1.3	3.2	7.9	87.3	1.6
Ti	0.0	0.1	99.3	0.5	0.0	0.0	98.9	1.1	0.0	0.0	98.1	1.9	0.0	13.9	33.3	52.8	0.0	4.4	20.6	75.0
Fe	0.0	10.8	88.9	0.3	0.0	24.7	71.1	4.1	0.0	11.2	86.2	2.6	1.0	2.0	54.7	42.3	0.1	1.3	33.6	65.0
Zr	1.9	87.1	10.1	0.9	0.8	93.4	3.8	2.0	1.1	90.9	7.8	0.3	0.7	95.8	3.4	0.1	0.5	95.9	3.4	0.1
Ga	0.0	0.0	99.8	0.1	0.2	0.0	99.8	0.0	0.0	0.0	99.9	0.1	0.6	23.5	55.6	20.4	0.5	4.3	59.1	36.0
Nb	0.0	0.6	98.7	0.7	0.1	0.4	99.4	0.1	0.0	0.6	99.1	0.3	0.1	0.2	94.6	5.1	0.0	0.0	98.6	1.3
In	2.6	3.9	92.1	1.3	1.2	3.5	93.0	2.3	4.0	12.0	80.0	4.0	6.7	66.7	20.0	6.7	17.6	58.8	17.6	5.9
Sn	0.4	2.1	95.8	1.7	0.4	1.6	96.9	1.2	0.7	2.6	94.1	2.6	1.6	8.1	83.9	6.5	1.9	5.7	83.0	9.4
Sb	0.4	0.6	98.8	0.2	1.1	1.6	96.9	0.4	0.2	0.5	99.1	0.2	0.8	74.4	24.0	0.8	0.7	41.6	56.6	1.1
Te	3.2	7.8	88.4	0.7	1.8	11.1	86.6	0.6	1.5	8.1	89.4	1.0	14.3	50.6	33.1	1.9	9.9	54.4	33.9	1.8
Hf	0.7	1.9	96.9	0.5	2.9	4.8	90.3	1.9	1.0	6.4	92.0	0.5	6.8	11.9	79.7	1.7	8.8	8.8	73.5	8.8
Ta	0.2	0.5	93.2	6.2	0.1	0.3	91.7	7.9	0.0	1.8	89.9	8.3	0.6	1.7	86.2	11.5	0.7	2.2	74.6	22.4
Bi	0.8	0.0	92.1	7.0	0.3	0.3	26.1	73.3	0.4	0.0	98.0	1.6	0.0	0.0	47.6	52.4	37.5	0.0	0.0	62.5
Th	0.1	0.1	99.3	0.6	0.1	21.6	74.7	3.6	0.0	0.0	99.7	0.2	0.2	0.7	92.0	7.1	0.3	0.9	87.2	11.6
V	0.5	33.1	66.3	0.2	0.6	71.4	26.6	1.3	0.3	21.7	77.4	0.7	7.2	82.4	9.6	0.8	6.3	78.8	11.4	3.5
Cr	2.1	4.1	89.6	4.1	1.4	1.8	92.6	4.1	2.2	3.3	88.9	5.6	2.0	9.7	85.0	3.2	1.9	2.9	92.0	3.2
As	0.2	0.6	99.2	0.1	1.5	1.2	97.0	0.3	0.0	0.4	99.2	0.4	1.7	2.5	95.3	0.5	1.0	1.5	86.0	11.5
Se	19.4	0.3	66.3	13.9	13.2	0.3	15.3	71.1	18.2	36.7	23.9	21.2	22.8	70.5	3.4	3.4	56.4	17.6	14.9	11.2
Mo	0.0	0.4	99.5	0.0	0.1	1.8	95.1	3.1	0.0	0.3	99.6	0.0	0.0	94.3	5.5	0.2	0.0	56.6	42.9	0.6
W	0.1	0.0	99.9	0.1	0.0	0.0	99.7	0.3	0.0	0.0	99.9	0.1	0.1	45.0	52.2	2.7	0.1	0.4	95.7	3.8

–, analytical data below limit of determination.

References

- Achterberg, E.P., Van den Berg, C.M.B., 1997. Chemical speciation of chromium and nickel in the western Mediterranean. *Deep-Sea Res. II* 44, 693–720.
- Aja, S.U., Wood, S.A., Williams-Jones, A.E., 1995. The aqueous geochemistry of Zr and the solubility of some Zr-bearing minerals. *Appl. Geochem.* 10, 603–620.
- Andreae, M.O., 1986. Chemical species in seawater and marine particulates. In: Bernhard, M., Brinckman, F.E., Sadler, P.J. (Eds.), *The Importance of Chemical 'Speciation' in Environmental Processes*. Dahlem Konferenzen, Springer, Berlin, pp. 301–335.
- Aplin, A.C., Cronan, D.S., 1985. Ferromanganese oxide deposits from the Central Pacific Ocean, I. Encrustations from the Line Islands Archipelago. *Geochim. Cosmochim. Acta* 49, 427–436.
- Au, K.-K., Penisson, A.C., Yang, S., O'Melia, C.R., 1999. Natural organic matter at oxide/water interfaces: Complexation and conformation. *Geochim. Cosmochim. Acta* 63, 2903–2917.
- Balistrieri, L.S., Brewer, P.G., Murray, J.W., 1981. Scavenging residence times of trace metals and surface chemistry of sinking particles in the deep ocean. *Deep-Sea Res.* 28 (2A), pp. 101–121.
- Balistrieri, L.S., Chao, T.T., 1990. Adsorption of selenium by amorphous iron oxyhydroxide and manganese dioxide. *Geochim. Cosmochim. Acta* 54, 739–751.
- Balistrieri, L.S., Murray, J.W., 1982. The surface chemistry of δ -MnO₂ in major ion seawater. *Geochim. Cosmochim. Acta* 46, 1041–1052.
- Belzile, N., Chen, Y.-W., Wang, Z., 2001. Oxidation of antimony (III) by amorphous iron and manganese oxyhydroxides. *Chem. Geol.* 174, 379–387.
- Bertine, K.K., Koide, M., Goldberg, E.D., 1996. Comparative marine chemistries of some trivalent metals – bismuth, rhodium and rare earth elements. *Mar. Chem.* 53, 89–100.
- Bidoglio, G., Gibson, P.N., O'Gorman, M., Roberts, K.J., 1993. X-ray absorption spectroscopy investigation of surface redox transformations of thallium and chromium on colloidal mineral oxides. *Geochim. Cosmochim. Acta* 57, 2389–2394.
- Bolton, B.R., Exon, N.F., Ostwald, J., Kudrass, H.R., 1988. Geochemistry of ferromanganese crusts and nodules from the south Tasman Rise, southeast of Australia. *Mar. Geol.* 84, 53–80.
- Bruland, K.W., 1983. Trace elements in seawater. In: Riley, J.P., Skirrow, G. (Eds.), *Chemical Oceanography*, Vol. 8. Academic Press, New York, pp. 157–220.
- Bruland, K.W., 1989. Oceanic zinc speciation: Complexation of zinc by natural organic ligands in the central North Pacific. *Limnol. Oceanogr.* 34, 267–285.
- Bruno, J., 1990. The influence of dissolved carbon dioxide on trace metal speciation in seawater. *Mar. Chem.* 30, 231–240.
- Byrne, R.H., 2002. Inorganic speciation of dissolved elements in seawater: The influence of pH on concentration ratios. *Geochem. Trans.* 2002 (2), http://www.rsc.org/CFmuscat/intermediate_abstract.cfm?FURL=/ej/gt/2002/B109732F/index.htm and TYP=EONLY.
- Byrne, R.H., Kump, L.R., Cantrell, K.J., 1988. The influence of temperature and pH on trace metal speciation in seawater. *Mar. Chem.* 25, 163–181.
- Cantrell, K.J., Byrne, R.H., 1987. Rare earth element complexation by carbonate and oxalate ions. *Geochim. Cosmochim. Acta* 51, 597–605.
- Chester, R., Hughes, M.J., 1967. A chemical technique for the separation of ferro-manganese minerals, carbonate minerals and adsorbed trace elements from pelagic sediments. *Chem. Geol.* 2, 249–269.
- Clegg, S.L., Sarmiento, J.L., 1989. The hydrolytic scavenging of metal ions by marine particulate matter. *Progr. Oceanogr.* 23, 1–21.
- Coale, K.H., Bruland, K.W., 1990. Spatial and temporal variability in copper complexation in the North Pacific. *Deep-Sea Res. I* 47, 317–336.
- Cowen, J.P., de Carlo, E.H., McGee, D.L., 1993. Calcareous nannofossil biostratigraphic dating of a ferromanganese crust from Schumann Seamount. *Mar. Geol.* 115, 289–306.
- De Carlo, E.H., Fraley, C.M., 1992. Chemistry and mineralogy of ferromanganese deposits from the equatorial Pacific Ocean. In: Keating, B.H., Bolton, B.R. (Eds.), *Geology and Offshore Mineral Resources of the Central Pacific Basin*. Circum-Pacific Council for Energy and Mineral Resources Earth Science Series 14, Springer, New York.
- De Carlo, E.H., Pennywell, P.A., Fraley, C.M., 1987. Geochemistry of ferromanganese deposits from the Kiribati and Tuvalu region of the west central Pacific Ocean. *Mar. Min.* 6, 301–321.
- De Vitre, R.R., Belzile, N., Tessier, A., 1991. Speciation and adsorption of arsenic on diagenetic iron oxyhydroxides. *Limnol. Oceanogr.* 36, 1480–1485.
- Djogic, R., Kniewald, G., Branica, M., 1988. Uranium in the marine environment. A geochemical approach to its hydrologic and sedimentary cycle, I. Theoretical considerations. In: Guary, J.C., Guegueniat, P., Pentreath, R.J. (Eds.), *Radionuclides: A Tool for Oceanography*. Elsevier Applied Science, Amsterdam, pp. 171–182.
- Donat, J.R., Bruland, W.K., 1995. Trace Elements in the Oceans. In: Salbu, B., Steinnes, E. (Eds.), *Trace Elements in Natural Waters*. CRC Press, Boca Raton, FL, pp. 247–281.
- Dzombak, D.A., Morel, F.M.M., 1990. *Surface Complexation Modelling – Hydrous Ferric Oxide*. Wiley, New York, 393 pp.
- Eisenhauer, A., Gögen, K., Pernicka, E., Mangini, A., 1992. Climatic influences on growth rates of Mn crusts during the Late Quaternary. *Earth Planet. Sci. Lett.* 109, 25–36.
- Flegal, A.R., Patterson, C.C., 1985. Thallium concentrations in seawater. *Mar. Chem.* 15, 327–331.
- Flegal, A.R., Sanudo-Wilhelmy, S., Fitzwater, S.E., 1989. Particulate thallium fluxes in the northeast Pacific. *Mar. Chem.* 28, 61–75.
- Förstner, U., Stoffers, P., 1981. Chemical fractionation of

- transition metals in Pacific pelagic sediment. *Geochim. Cosmochim. Acta* 45, 141–146.
- François, R., Honjo, S., Krishfield, R., Manganini, S., 2002. Running the gauntlet in the twilight zone: The effect of midwater processes on the biological pump. *US JGOFs Newslett.* 11, 4–6.
- Frank, M., O’Nions, R.K., Hein, J.R., Banakar, V.K., 1999. 60 Myr records of major elements and Pb–Nd isotopes from hydrogenous ferromanganese crusts: Reconstructions of seawater paleochemistry. *Geochim. Cosmochim. Acta* 63, 1689–1708.
- Fry, B., Peltzer, E.T., Hopkinson, C.S., Jr., Nolin, A., Redmond, L., 1996. Analysis of marine DOC using a dry combustion method. *Mar. Chem.* 54, 191–201.
- Giovanoli, R., Arrhenius, G., 1988. Structural chemistry of marine manganese and iron minerals and synthetic model compounds. In: Halbach, P., Friedrich, G., von Stackelberg, U. (Eds.), *The Manganese Nodule Belt of the Pacific Ocean*. Enke, Stuttgart, pp. 20–37.
- Glasby, G.P., Stüben, D., Jeschke, G., Stoffers, P., Garbeschönber, C.-D., 1997. A model for the formation of hydrothermal manganese crusts from the Pitcairn Island hotspot. *Geochim. Cosmochim. Acta* 61, 4583–4597.
- Goldberg, E.D., Koide, M., Schmitt, R.A., Smith, R.H., 1963. Rare-earth distribution in the marine environment. *J. Geophys. Res.* 68, 4209–4217.
- Halbach, P., 1986. Processes controlling the heavy metal distribution in Pacific ferromanganese nodules and crusts. *Geol. Rundsch.* 75, 235–247.
- Hein, J.R., Morgan, C.L., 1999. Influence of substrate rocks on Fe–Mn crust composition. *Deep-Sea Res. I* 46, 855–875.
- Hein, J.R., Hsueh Wen, Y., Gunn, S.H., Sliter, W.V., Benninger, L.M., Wang, C.-H., 1993. Two major Cenozoic episodes of phosphogenesis recorded in equatorial Pacific seamount deposits. *Paleoceanography* 8, 293–311.
- Hein, J.R., Koschinsky, A., Halliday, A.N., 2003. Global occurrence of tellurium-rich ferromanganese crusts and a model for the enrichment of tellurium. *Geochim. Cosmochim. Acta* 67, 1117–1127.
- Hein, J.R., Koschinsky, A., Bau, M., Manheim, F.T., Kang, J.K., Roberts, L., 2000. Cobalt-rich ferromanganese crusts in the Pacific. In: Cronan, D. (Ed.), *Handbook of Marine Mineral Deposits*. CRC Press, Boca Raton, FL, pp. 239–279.
- Hein, J.R., Koschinsky, A., Halbach, P.E., Manheim, F.T., Bau, M., Kang, J.K., Lubick, N., 1997. Iron and manganese oxide mineralization in the Pacific. In: Nicholson, K., Hein, J.R., Bühn, B., Dasgupta, S. (Eds.), *Manganese Mineralization: Geochemistry and Mineralogy of Terrestrial and Marine Deposits*. Geological Society Special Publications 119, 123–138.
- Hodkinson, R.A., Stoffers, P., Scholten, J., Cronan, D.S., Jeschke, G., Rogers, T.D.S., 1994. Geochemistry of hydrothermal manganese deposits from the Pitcairn Island hotspot, southeastern Pacific. *Geochim. Cosmochim. Acta* 58, 5011–5029.
- Hunter, K.A., Liss, P.S., 1979. The surface charge of suspended particles in estuarine and coastal waters. *Nature* 282, 823–825.
- Ingram, B.L., Hein, J.R., Farmer, G.L., 1990. Age determinations and growth rates of Pacific ferromanganese deposits using strontium isotopes. *Geochim. Cosmochim. Acta* 54, 1709–1721.
- James, R.O., Healy, T.W., 1972. Adsorption of hydrolyzable metal ions at the oxide–water interface, III. Thermodynamic model of adsorption. *J. Colloid Interface Sci.* 40, 65–81.
- Jeandel, C., Caisso, M., Minster, J.F., 1987. Vanadium behaviour in the global ocean and in the Mediterranean Sea. *Mar. Chem.* 21, 51–74.
- Kersten, M., Förstner, U., 1989. Speciation of trace elements in sediments. In: Batley, G.E. (Ed.), *Trace Element Speciation: Analytical Methods and Problems*. CRC Press, Boca Raton, FL, pp. 245–309.
- Klován, J.E., Imbrie, J., 1971. An algorithm and FORTRAN-IV program for large-scale Q-mode factor analysis and calculation of factor scores. *Math. Geol.* 3, 61–77.
- Koschinsky, A., Halbach, P., 1995. Sequential leaching of marine ferromanganese precipitates: Genetic implications. *Geochim. Cosmochim. Acta* 59, 5113–5132.
- Koschinsky, A., Stascheit, A., Bau, M., Halbach, P., 1997. Effects of phosphatization on the geochemical and mineralogical composition of marine ferromanganese crusts. *Geochim. Cosmochim. Acta* 61, 4079–4094.
- Koschinsky, A., Van Gerven, M., Halbach, P., 1995. First investigations of massive ferromanganese crusts in the NE Atlantic in comparison with hydrogenetic Pacific occurrences. *Mar. Geores. Geotechn.* 13, 375–391.
- Kosmulski, M., 2002. The pH-dependent surface charging and the points of zero charge. *J. Colloid Interface Sci.* 253, 77–87.
- Kuhn, T., Bostwick, B.C., Koschinsky, A., Halbach, P., Fendorf, S., 2003. Unusual enrichment of Mo in hydrothermal Mn precipitates: Possible sources, formation and phase associations. *Chem. Geol.* 199, 31–45.
- Kuma, K., Usui, A., Paplawsky, W., Gedulin, B., Arrhenius, G., 1994. Crystal structure of synthetic 7Å and 10Å manganese substituted by mono- and divalent cations. *Mineral. Mag.* 58, 425–447.
- Kusakabe, M., Ku, T.L., 1984. Incorporation of Be isotopes and other trace metals into marine ferromanganese deposits. *Geochim. Cosmochim. Acta* 48, 2187–2193.
- Lee, D.S., Edmond, J.M., 1985. Tellurium species in seawater. *Nature* 313, 782–785.
- Li, Y.-H., 1981. Ultimate removal mechanisms of elements from the ocean. *Geochim. Cosmochim. Acta* 45, 1659–1664.
- Li, Y.-H., 1982. Interelement relationship in abyssal Pacific ferromanganese nodules and associated pelagic sediments. *Geochim. Cosmochim. Acta* 46, 1053–1060.
- Li, Y.-H., 1991. Distribution patterns of the elements in the ocean: A synthesis. *Geochim. Cosmochim. Acta* 55, 3223–3240.
- Manceau, A., Gorshkov, A.I., Drits, V.A., 1992. Structural chemistry of Mn, Fe, Co, and Ni in manganese hydrous oxides, Part II. Information from EXAFS spectroscopy

- and electron and X-ray diffraction. *Am. Mineral.* 77, 1144–1157.
- Measures, C.I., Grant, B., Khadem, M., Lee, D.S., Edmond, J.M., 1984. Distribution of Be, Al, Se, Bi in the surface waters of the western North Atlantic and Caribbean. *Earth Planet. Sci. Lett.* 71, 1–12.
- Millero, F., 1990. Marine solution chemistry and ionic interactions. *Mar. Chem.* 30, 205–229.
- Millero, F., 2001. Speciation of metals in natural waters. *Geochem. Trans.* 2001 (8), http://www.rsc.org/CFmuscat/intermediate_pubs.cfm?FURL=/ej/gt/2001/B104809K/index.htm and TYP=EONLY.
- Mills, R.A., Wells, D.M., Robert, S., 2001. Genesis of ferromanganese crusts from the TAG hydrothermal field. *Chem. Geol.* 176, 283–293.
- Moorby, S.A., Cronan, D.S., 1981. The distribution of elements between co-existing phases in some marine ferromanganese-oxide deposits. *Geochim. Cosmochim. Acta* 45, 1855–1877.
- Morford, J.L., Emerson, S., 1999. The geochemistry of redox sensitive trace metals in sediments. *Geochim. Cosmochim. Acta* 63, 1735–1750.
- Murphy, E., McMurtry, G.M., Kim, K.H., DeCarlo, E.H., 1991. Geochemistry and geochronology of a hydrothermal ferromanganese deposit from the North Fiji Basin. *Mar. Geol.* 98, 297–312.
- Murray, J.W., Dillard, J.G., 1979. The oxidation of cobalt(II) adsorbed on manganese dioxide. *Geochim. Cosmochim. Acta* 43, 781–788.
- Murray, D.J., Healy, T.W., Fuerstenau, D.W., 1968. The adsorption of aqueous metal on colloidal hydrous manganese oxide. *Adv. Chem.* 79, 74–81.
- Nathan, Y., 1984. The mineralogy and geochemistry of phosphorites. In: Nriagu, J.O., Moore, P.B. (Eds.), *Phosphate Minerals*. Springer, pp. 275–288.
- Nriagu, J.O., 1984. Formation and stability of base metal phosphates in soils and sediments. In: Nriagu, J.O., Moore, P.B. (Eds.), *Phosphate Minerals*. Springer, pp. 319–329.
- Orians, K.J., Boyle, E.A., Bruland, K.W., 1990. Dissolved titanium in the open ocean. *Nature* 348, 322–325.
- Oscarson, D.W., Huang, P.M., Defosse, C., Herbillon, A., 1981. Oxidative power of Mn(IV) and Fe(III) oxides with respect to As(III) in terrestrial and aquatic environments. *Nature* 291, 50–51.
- Pichocki, C., Hoffert, M., 1987. Characteristics of Co-rich ferromanganese nodules and crusts sampled in French Polynesia. *Mar. Geol.* 77, 109–119.
- Piper, D.Z., 1974. Rare earth elements in ferromanganese nodules and other marine phases. *Geochim. Cosmochim. Acta* 38, 1007–1022.
- Pujing, P., Susak, N.J., 1991. The speciation of cobalt in seawater and fresh waters at 25 degrees C. *Geochem. J.* 25, 411–420.
- Puteanus, D., Halbach, P., 1984. Correlation of Co concentration and growth rate – A method for age determination of ferromanganese crusts. *Chem. Geol.* 69, 73–85.
- Sadiq, M., 1990. Arsenic chemistry in marine environments: A comparison between theoretical and field observations. *Mar. Chem.* 31, 285–297.
- Sander, S., Koschinsky, A., 2000. Onboard-ship redox speciation of chromium in diffuse hydrothermal fluids from the North Fiji Basin. *Mar. Chem.* 71, 83–102.
- Sato, Y., Okabe, S., Takematsu, N., 1989. Major elements in manganese and iron oxides precipitated from seawater. *Geochim. Cosmochim. Acta* 53, 1883–1887.
- Schedlbauer, O.F., Heumann, K.G., 2000. Biomethylation of thallium by bacteria and first determination of biogenic dimethylthallium in the ocean. *Appl. Organomet. Chem.* 14, 330–340.
- Schindler, P.W., 1981. Surface complexes at oxide–water interfaces. In: Anderson, M.A., Rubin, A.J. (Eds.), *Adsorption of Inorganics at Solid–Liquid Interface*. Ann Arbor Science, Ann Arbor, pp. 1–49.
- Segl, M., Mangini, A., Bonani, G., Hofmann, H.J., Nessi, M., Suter, M., Wölfi, W., Friedrich, G., Plüger, W.L., Wiechowski, A., Beer, J., 1984. ¹⁰Be dating of a manganese crust from Central North Pacific and implications for ocean palaeocirculation. *Nature* 309, 540–543.
- Smedley, P.L., Kinniburgh, D.G., 2002. A review of the source, behaviour and distribution of arsenic in natural waters. *Appl. Geochem.* 17, 517–568.
- Sohrin, Y., Fujishima, Y., Ueda, K., Akiyama, S., Mori, K., Hasegawa, H., Matsui, M., 1998. Dissolved niobium and tantalum in the North Pacific. *Geophys. Res. Lett.* 25, 999–1002.
- Sohrin, Y., Matsui, M., Nakayama, E., 1999. Contrasting behaviour of tungsten and molybdenum in the Okinawa Trough, the East China Sea and the Yellow Sea. *Geochim. Cosmochim. Acta* 63, 3457–3466.
- Sposito, G., 1983. On the surface complexation model of the oxide–aqueous solution interface. *J. Colloid Interface Sci.* 91, 329–340.
- Stanley, J.K., Byrne, R.H., 1990. Inorganic complexation of Zinc(II) in seawater. *Geochim. Cosmochim. Acta* 54, 753–760.
- Stumm, W., 1992. *Chemistry of the Solid–Water Interface*. Wiley, New York.
- Stumm, W., Kummert, R., Sigg, L., 1980. A ligand exchange model for the adsorption of inorganic and organic ligands at hydrous oxide interfaces. *Croat. Chem. Acta* 53, 291–312.
- Stumm, W., Morgan, J.J., 1996. *Aquatic Chemistry*, 3rd ed. Wiley, New York.
- Takematsu, N., Sato, Y., Okabe, S., Nakayama, E., 1985. The partition of vanadium and molybdenum between manganese oxides and sea-water. *Geochim. Cosmochim. Acta* 49, 2395–2399.
- Takematsu, N., Sato, Y., Okabe, S., Usui, A., 1990. Uptake of selenium and other oxyanionic elements in marine ferromanganese concretions of different origin. *Mar. Chem.* 31, 271–283.
- Tipping, E., Hetherington, N.B., Hilton, J., Thompson, D.W., Bowles, E., Hamilton-Taylor, J., 1985. Artefacts in the use of selective chemical extraction to determine distributions of

- metals between manganese and iron. *Anal. Chem.* 57, 1944–1946.
- Tripathy, S.S., Kanungo, S.B., Mishra, S.K., 2001. The electrical double layer at hydrous manganese dioxide/electrolyte interface. *J. Colloid Interface Sci.* 241, 112–119.
- Turner, D.R., Whitfield, M., Dickson, A.G., 1981. The equilibrium speciation of dissolved components in freshwater and seawater at 25°C and 1 atm pressure. *Geochim. Cosmochim. Acta* 45, 855–881.
- Usui, A., Mellin, T.A., Nohara, M., Yuasa, M., 1989. Structural stability of marine 10Å manganates from the Ogasawara (Bonin) Arc: implication for low-temperature hydrothermal activity. *Mar. Geol.* 86, 41–56.
- Usui, A., Someya, M., 1997. Distribution and composition of marine hydrogenetic and hydrothermal manganese deposits in the northwest Pacific. In: Nicholson, K., Hein, J.R., Böhn, B., Dasgupta, S. (Eds.), *Manganese Mineralization: Geochemistry and Mineralogy of Terrestrial and Marine Deposits*. Geological Society Special Publications 119, 123–138.
- Van den Berg, C.G.M., 1995. Evidence for organic complexation of iron in seawater. *Mar. Chem.* 50, 139–157.
- Von Damm, K.L., 1995. Controls on the chemistry and temporal variability of seafloor hydrothermal fluids. In: Humphris, S.E., Zierenberg, R.A., Mullineaux, L.S., Thomson, R.E. (Eds.), *Seafloor Hydrothermal Systems: Physical, Chemical, Biological, and Geological Interactions*. Geophysical Monograph 91, American Geophysical Union, pp. 222–247.
- Wehrli, B., Stumm, W., 1989. Vanadyl in natural waters: Adsorption and hydrolysis promote oxygenation. *Geochim. Cosmochim. Acta* 53, 69–77.
- Wehrli, B., Sulzberger, B., Stumm, W., 1989. Redox processes catalyzed by hydrous oxide surfaces. *Chem. Geol.* 78, 167–179.